NUMERICAL STUDY OF A CAPACITIVE TOMOGRAPHY SYSTEM FOR MULTIPHASE FLOW

L. F. M. Moura,
E. Cenedese
and A. C. Azevedo Filho

Universidade Estadual de Campinas
Faculdade de Engenharia Mecânica
Departamento de Engenharia Térmica e de Fluidos
Cidade Universitária "Zeferino Vaz"
Distrito de Barão Geraldo
P.O Box 6122, Campinas, São Paulo, Brasil
felipe@fem.unicamp.br

ABSTRACT

This paper presents the development of a capacitive tomography system applied to the study of multiphase flows. A numerical analysis, through the finite elements method, was performed to obtain data for the optimization of the geometry of the capacitance sensor. The image reconstruction of several flow patterns was obtained through the method of linear back projection, allowing the verification of the influence of several parameters upon the quality of the images, making its application easier in an experimental procedure. Several numerical simulations were performed for air-water flow, for the stratified and annular patterns. A resource of cut-off level, which depends of previous knowledge of the liquid fraction, was implemented in a way to improve the quality of the reconstructed images. The results obtained for several values of void fraction and for different patterns of flow, demonstrate the validity of the developed tomographic system.

Keywords: Tomography, Multiphase Flows, Capacitance Sensor, Image Reconstruction, Linear Back Projection.

NOMENCLATURE

$C_{i,j}$ capacitance between the pair of electrodes i-j
C_v volumetric fraction of dispersed phase

Greek symbols

Γ_j area of the sensor electrode
ε_1 relative permittivity of phase
ε_2 relative permittivity of phase
ε_m relative permittivity of the mixture
$\varepsilon_r(x,y)$ relative permittivity
ε_0 absolute permittivity of vacuum
$\phi(x,y)$ electric potential
ϕ_j electric potential in the sensor electrode
$\phi_i(x,y)$ distribution of the electric potential when the electrode i is the emitter electrode
ϕ_I electric potential in the emitter electrode

INTRODUCTION

The main purpose of tomography is to obtain an image (bidimensional or tridimensional) of an object (parts of the human body, multiphase flow, etc.) Through the processing of signals sent and received by sensors located around the object that an image is needed.

Some reports about the tomography were written near 1826 by a Norwegian physician called Abel. However only around 1970 it appeared an image reconstruction technique of the internal organs of the human body, called computed tomography. The image reconstruction techniques in medical tomography got a huge boost from the development of an image reconstruction algorithm, called the filtered backprojection algorithm, by Bracewell and Riddle (1967). Later, Ramanchandran and Lakshinarayanan (1971) also developed papers about the filtered backprojection algorithm where it was applied the convolution theory instead of the Fourier transformation.

Around the 80's the tomography was no more restrict only to the medical area and started to have a series of industrial applications, like in the control and monitoring of industrial processes known as Process Tomography (PT) or yet as Industrial Process Tomography (IPT).

The application of the tomography in industrial processes promoted the appearance of a great variety of tomographic techniques. For industrial applications that aim the monitoring and control of dynamic processes, it was observed that the slow response of the radiation detectors, as well as the slowness of the sequential movements of nucleonic tomography (that uses X rays or gamma rays), render these techniques indicated only for the obtainment of images of stationary objects, do not providing for the objectives of industrial tomography, because it does not possess temporal resolution for such measurements. To overcome the problems of temporal resolution it appears the tomography that uses electrical or magnetic properties. Among them, the electrical capacitance tomography is emphasized because, when compared to the other techniques, it possesses the following advantages: low cost, quick responses and it is not dangerous to health like the X rays and gamma rays. The electrical capacitance tomography can also overcome several problems associated to the application of intrusive sensors. This

technique is adequate to the problems where it exist components with different relative electrical permittivity, and it can be used including for non conductive components. The using of capacitance sensors for the monitoring of industrial processes started to be studied near 1950.

Before presenting more specific considerations about the tomography, it is necessary to discourse about the multiphase flows and its characteristics, such as the flow patterns and its interfaces. A more detailed explanation about these flows is justified by the fact of this paper to be directed to tomography with industrial applications, with the purpose to monitor the flow and to identify the flow patterns and the interfaces of a multiphase mixture.

The multiphase flow is a constant presence in most equipment and industrial processes, especially in the ones that deal with electric power generation, refrigeration and distilling. Among these equipment and processes it is found several types of multiphase flows, such as: gas and solid particles; gas and solid drops; liquid and air bubbles; liquid and solid particles.

The study of multiphase flows faces, initially, one of its main characteristics: a mobile and deformable region, common to the phases, called interface. The interface is a region of extreme importance in the study of multiphase flows, because it is in this region where the mass, momentum and heat transfer are processed. The interfaces may be continuous, like the case of annular and stratified flow, as may appears in a discontinuous manner in great quantities and totally scattered, like in the case of disperse flow.

Ishii (1975) divided the two-phase flows in classes that divide in patterns, distinguishing one from the others regarding to the interface geometry. In function of the interface shape, he proposed three major classes: disperse phase flow, flow of separated phases and flow in transition.

There is a great variety of tomographic techniques that are applied for the image reconstruction both in the medical tomography and in the multiphase processes tomography. All tomographic techniques used have always in common the sending and the acquisition of signals from the devices that are located all around the object that it is imaged. In this paper it is developed an electrical capacitance tomography system for application in industrial processes.

CAPACITAVE TOMOGRAPHY FOR MULTIPHASE FLOW

The electrical capacitance tomography technique is adequate to processes in which the phases present different relative electrical permittivities, and it can be conductors or not conductors. The base of any tomography resides in explore the differences or contrasts in the properties of the process to be studied. The capacitance sensors are sensible to differences of relative electrical permittivity, while the X rays and the gamma rays are sensible to difference of density.

The theoretic model relating the electrical impedance or the relative permittivity of a two-phase mixture with a phase dispersed in a continuous phase was first presented by Maxwell in 1873. The theory of Maxwell stated that little spheres of a specific material were disseminated in a continuous phase and that the electrical field was disturbed by the presence of the spheres. In its theory, Maxwell assumed the spheres as being of equal size and small compared with the distance between them and formulated the relative permittivity of the mixture according to the equation:

$$\varepsilon_m = \varepsilon_1 \frac{2\varepsilon_1 + \varepsilon_2 - 2C_v(\varepsilon_1 - \varepsilon_2)}{2\varepsilon_1 + \varepsilon_2 + C_v(\varepsilon_1 - \varepsilon_2)} \quad (1)$$

According to Geldart and Kelsley (1972) and Hage and Werther (1997), the determination of relative permittivity of a multiphase mixture using the concepts of Maxwell is used still today in the monitoring of gas-solid, gas-liquid and liquid-solid systems.

The electric tomography, especially by capacitance, allows to overcome several problems associated to the application of intrusive sensors, as also allows a detailed analysis of the morphology of a multiphase flow. When the amount or how the phases are arranged in the interior of a capacitance sensor varies, it occur a variation of the relative permittivity of the medium and a consequent of capacitance. It's based on these variations that dwell the basic idea of electric capacitance tomography, which is the reconstruction of interface that separates the phases of a multiphase mixture from the capacitance measurements between different pairs of electrodes, associated to some algorithm of image reconstruction

According to Dykesteen et al (1985) and Strizzolo and Convenrti (1993), the simpler type of capacitance sensor to measure the phase concentration consist of two copper plates placed diametrically opposed in the external surface of the wall of a tube of nonconductive material

According to Yang and York (1999), the electric capacitance tomography system, when compared to other systems, has the following advantages: non invasive, low cost, quick responses, non-health threatening. Still according to the authors, some electric capacitance tomography systems, using sensors with 12 electrodes, can collect sufficient data to produce 40 images by second in an online system

ALGORITHMS FOR IMAGE RECONSTRUCTION

For the image reconstruction from the capacitance measurements it is necessary to use

mathematical algorithms that aids in the reconstitution of spatial distribution of relative permittivity of the phases. For this purpose, a diversity of iterative and non iterative algorithms has been created. Some of these algorithms received improvements or were adapted for the process tomography.

The more common algorithms used in image reconstruction for electric capacitance tomography are: reconstruction based on models, algebraic reconstruction, use of consultation tables, artificial neural networks, simultaneous iterative reconstruction and linear backprojection. This last one will be used in this work.

The objective of the image reconstruction is to calculate the relative permittivity of each one of the pixels from all possible capacitance measurements, in other words, to determine which phase occupies each pixel. However, this can not be done directly because there is no sufficient information. Therefore, it's customary to use a second set of data, known as sensibility map, that may be obtained through the measurements or numerical simulations for a given sensor. The image is then reconstructed combining the capacitance measurements between the pairs of electrodes with the weighting factors of each pixel (coefficients of the sensibility map).

According to Xie et al. (1993), Nooralahiyan et al (1993), Mc Kee et al (1993) and Fasching and Smith (1991), the algorithm of linear backprojection is an algorithm typically qualitative and not iterative, being an appropriated technique for the use in real time due to its computational simplicity.

NUMERICAL MODEL

It's described here the procedure adopted in numerical simulations, where it will be investigated the variation of the capacitance values as a function of some physical parameters of the sensor and the spatial distribution of phases in the interior of the sensor. The numerical simulation offers an indispensable resource to the image reconstruction, in regard to obtaining the sensibility map from the capacitance values for the several pairs of electrodes.

The sensor used in the numerical simulations is composed by a acrylic tube having in its exterior surface eight electrodes equally spaced and all this entire set is involved by a protection called shield. A scheme of the cross section of the sensor is presented in the figure 1.

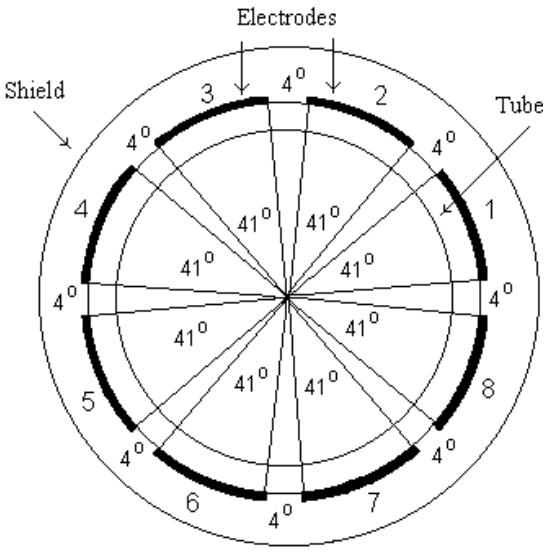

Figure 1. Scheme of the cross section of the capacitance sensor.

The image reconstruction of multiphase flow patterns using electric capacitance tomography means to represent the distribution of relative permittivity of the phases in a bidimensional plan, in other words, to reconstruct the spatial distribution of phases. With a capacitance sensor composed by n electrodes can be obtained $n(n-1)/2$ independent capacitance measurements between the electrode pairs, for a given situation Thus, with a sensor composed by eight electrodes it's possible to obtain 28 independent capacitance measurements. The image reconstruction in a capacitance tomography system involves two steps: the direct problem and the indirect problem.

The direct problem is to obtain all possible capacitance values between the pairs of electrode, for a given distribution of phases in the interior of the sensor. The solution of the direct problem consists in solving the elliptic partial differential equation of second order representing the electrical potential (Gauss law), known as Laplace equation:

$$\nabla.[\varepsilon_0 \cdot \varepsilon_r(x,y)\nabla\phi(x,y)]=0 \qquad (2a)$$

$$\nabla^2\phi(x,y)+\frac{1}{\varepsilon_r(x,y)}\cdot \text{grad}\phi(x,y)\cdot \text{grad}\varepsilon_r(x,y)=0 \qquad (2b)$$

(ε_0 = 8.854 pF/m).

Once obtained the distribution of the electric potential in the interior of the sensor, the capacitance can be determined through the equation:

$$C_{i,j}=\frac{\varepsilon_0}{(\phi_i-\phi_j)}\int_{(x,y)\in\Gamma j}\varepsilon_r(x,y)\nabla\phi_i(x,y).d\Gamma_j \qquad (3)$$

For a uniform distribution of relative permittivity we have $\text{grad}(\varepsilon_r(x,y))=0$ and the equation (2) is reduced to the equation (4) and the equation (3) is reduced to the equation (5). In the tomography applied to the multiphase flows, this case represents the sensor filled with only one of the phases.

$$\nabla^2\phi(x,y)=0 \tag{4}$$

$$C_{i,j}=\varepsilon_r(x,y)C_0=C_0\frac{\varepsilon_0}{(\phi_i-\phi_j)}\int_{(x,y)\in\Gamma j}\nabla\phi_i(x,y).d\Gamma_j \tag{5}$$

Equation (1a) can only be resolved analytically for simple cases. That is why the finite elements method is usually used to determine the capacitance values between the pairs of electrodes. Belo (1995) presents an analytical solution for the case where the emitter and sensor electrodes form any angle.

The inverse problem is to determine the spatial distribution of the relative permittivities (or the phases) from the capacitance measurements, that is, the inverse of the equation (2). The distribution of electric potential is implicitly dependent of the distribution of permittivity, as can be observed in the equation (1a). But, due to the irregularity in the potential distribution, there is no analytical solution for the equation (2) and numerical solutions are obtained through the finite elements method.

The solution found to obtain the images of the relative permittivity distribution, without the need to solve the equation (2) in its inverse form, was the establishment of a relation between the capacitance values and a sensibility map (obtained numerically) for each pair of electrode. Through this relation it raises a variable designated as gray level, which expresses a representative value of the relative permittivity in each pixel, as a function of the capacitance measurements between the pairs of electrode, for a specific phase distribution. In this work we used the linear backprojection method for the calculation of the gray level of the pixels for a specific phase distribution. The values of the gray level of the pixels are then used to represent a flow image.

The quality of the images can be improved using a feature called cut-off level. In this case we need to know the true value of the liquid fraction (βv) of the multiphase flow as input variable, also called of input liquid fraction.

Once calculated the gray level for each pixel it's possible to establish the liquid fraction without cut-off level (βsc). This value is calculated adding up the values of gray level of all pixels and dividing this sum by the total numbers of pixels.

The liquid fraction with cut-off level (βcc) is obtained in an iterative way, adding up the values of gray level of all pixels contained in the liquid phase and dividing by the total number of pixels. The value of the cut-off level is updated at each iteration and the value of βcc is compared with the value of the input liquid fraction (βv), until the difference between these values is less than a tolerance previously established. Once established the final value of the cut-off level, the interface between the phases can be defined in the following manner: all pixels that have a gray level value below to above to the cut-off level will be equal to 1.

The images reconstructed using the feature of cut-off level present an outline of the interface well defined. In the other hand, the images reconstructed without this feature exhibit the change of a phase to another in a soft form, complicating the interpretation of the image with regard to identification of the flow pattern and the location of the interface. The detailed procedure of the algorithm of linear backprojection for the image reconstruction, with the feature of cut-off level, can be found in Azevedo Filho (2002).

OPTIMIZATION OF THE SENSOR GEOMETRY

In order to obtain the better geometry for the capacitance sensor, several numerical simulations were performed with the software ansys, for a bidimensional geometry representing the transversal section of the sensor.

For the generation of the mesh, the domain was divided in eight sectors, where each sector comprehends a partition of 45°, in other words 1/8 of the circumference. Each sector was divided in three regions in the radial direction: an internal region where the fluids are flowing, a intermediary region that corresponds to the tube wall and a external region between the shield and the external surface of the tube. The eight electrodes are placed in the external surface of the tube in each of the eight sectors. each of these regions is composed by several layers formed by finite triangular elements of three knots. At the emitter and sensor electrodes, it's applied the boundary conditions of electric potential equal to 1 and 0, respectively. For the free electrodes (that aren't emitter neither sensor) two different boundary conditions were used: grounded free electrodes (potential equals to 0) and floating free electrodes (without specifying the potential value). These two conditions correspond to the two techniques of capacitance measurement.

The main characteristics of the capacitance sensor are: material of the tube; internal and external radius of the tube; quantity, angle and length of the electrodes; and radius of the shield. The variation of any of these characteristics influences in the capacitance values. The numerical simulations were performed varying some of these parameters. In order to compare the numerical results, a standard geometry of the sensor was defined: a tube of acrylic (relative permittivity equal to 3,0) with internal radius

of 26.35 mm and external radius of 30.0 mm (thickness of the wall equals to 3.65mm). The standard sensor has eight electrodes placed in the external wall of the tube, with equal space between them, and each electrode has an angle of 41^o and a length of 100 mm. The distance between the external surface of the tube and the shield was considered as being equal to 15mm. The relative permittivity of the water and the air were considered as being equal to 80 and 1 respectively.

In the optimization process of the capacitance sensor geometry, the influence of the following parameters on the capacitance values was investigated: electrode angle; relative permittivity and thickness of the tube wall. The numerical simulations were performed for the sensor full of water and full of air, for the case of floating free electrodes, since the numerical simulations for the case of grounded free electrodes is described in Azevedo Filho (2002). The comparisons were made always considering the geometry of the standard sensor.

Figure 2 show the capacitance values as a function of the electrode angle, with the tube filled with water and air for floating free electrodes. It is observed for that decreasing the electrode angle decreases the capacitance values for all pairs of electrodes, but the capacitance of the pair (1,2), with the tube filled with water for the floating case, is the one that suffers more influence.

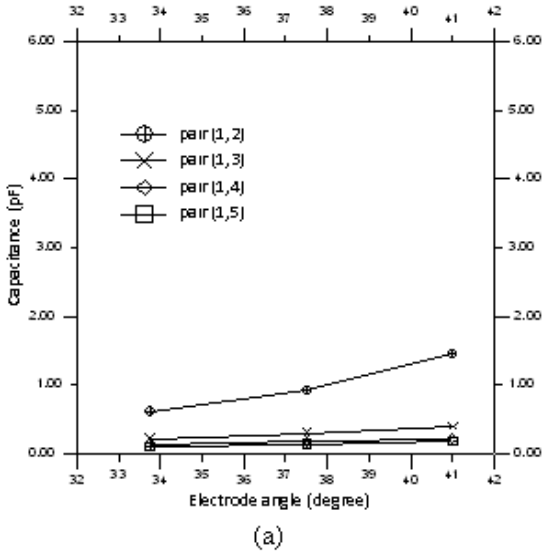

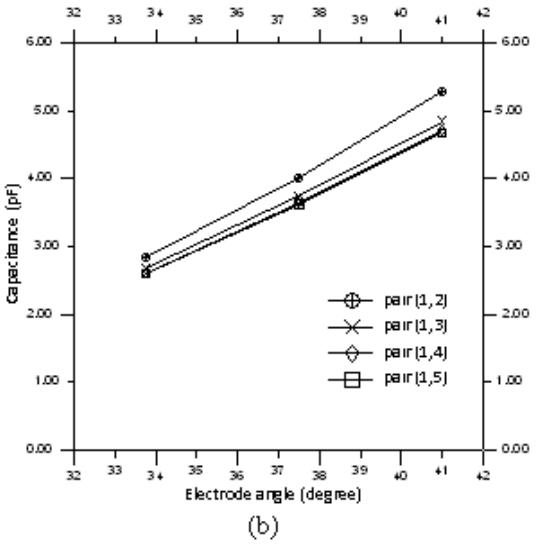

Figure 2. Capacitance values as a function of the electrode angle, for floating free electrodes, with (a) the sensor filled with air and (b) the sensor filled with water

Figure 3 show the capacitance values as a function of the tube relative permittivity, with the tube filled with water and filled with air for floating free electrodes. It is observed that increasing the tube relative permittivity increases the capacitance values for all pairs of electrodes and the capacitance of the pair (1,2) with the tube filled with water, for the floating free electrodes, is the one that suffers more influence.

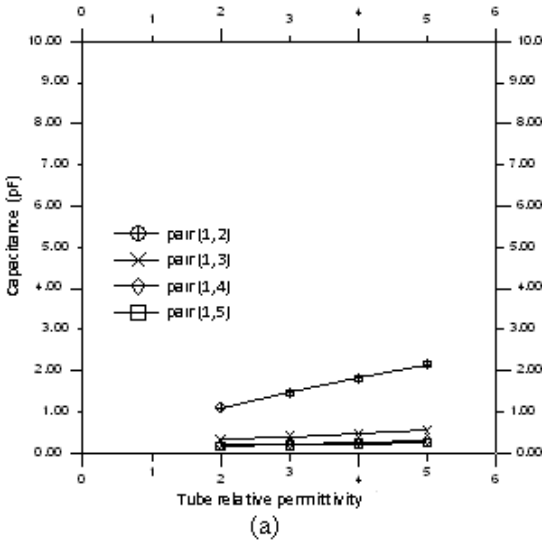

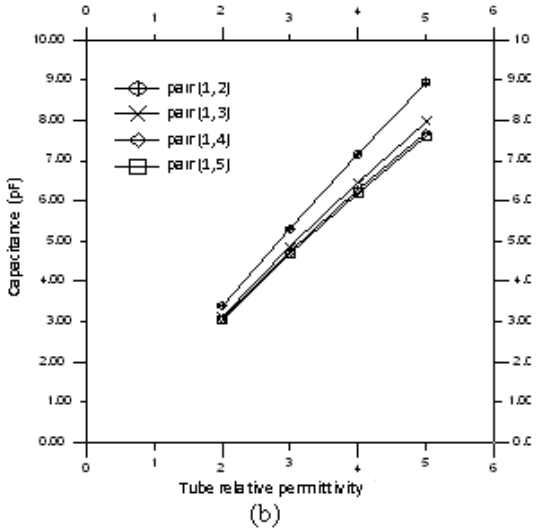

Figure 3. capacitance values as a function of the tube relative permittivity, for floating free electrodes, with (a) the sensor filled with air and (b) the sensor filled with water

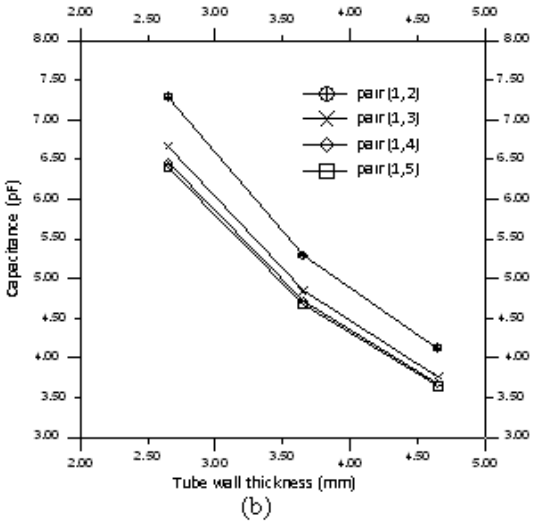

Figure 4. Capacitance values as a function of the tube wall thickness, for the case of floating free electrodes, with (a) the sensor filled with air and (b) the sensor filled with water

Figure 4 show the capacitance values as a function of the tube wall thickness, for the tube filled with water and filled with air for floating free electrodes. It can be observed that, in the case of the sensor filled with air, increasing the tube wall thickness does not have a great influence over the capacitance values for floating free electrodes. In the case of the sensor filled with water, the increase in the tube wall thickness decreases significantly the capacitance values, for floating free electrodes.

For the three analyzed cases, it can be observed yet a significant difference between the capacitance values for the sensor filled with air and water this difference, also known as contrast, is highly desirable because allows to differentiate a phase of another one during the image reconstruction process.

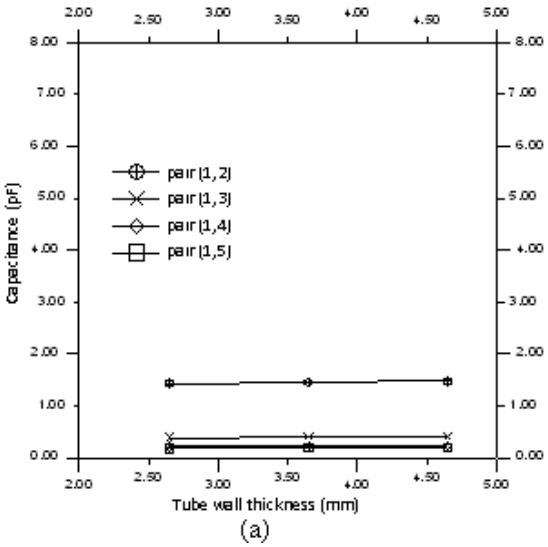

A criterion for optimizing the geometry of the sensor is the ratio between the capacitance of the pair of electrodes (1,2) for the sensor filled with the phase of higher relative permittivity and the capacitance of the pair of electrodes (1,5) for the sensor filled with the phase of lower relative permittivity. From the results of the numerical simulations presented above, it can be observed that the variation of the electrode angle strongly influences the capacitance values of all pairs of electrodes, for of floating free electrodes. This influence is observed with more intensity for floating free electrodes with sensor filled with water. The numerical simulation results show yet that increasing the electrode angle increases the capacitance values for the pairs of electrodes (1,4) and (1,5). These pairs of electrodes usually are the ones that present the lowest capacitance values, demanding more sensible capacitance measuring systems.

The variations of the relative permittivity and the wall thickness of the tube have influence in the capacitance values of the pair of electrodes (1,4) and (1,5) for flouting free electrodes with the sensor filled with air. Despite of the relative influence of permittivity and wall thickness of the tube in the capacitance values, we cannot consider these parameters in the optimization process of sensor geometry, since these characteristics are previously defined in the choosing of the tube

Then, two criteria were defined for the optimization of the parameters of the capacitance sensor. The highest possible value of the capacitance for the pair of electrodes (1,5) with the tube filled with the phase of lower relative permittivity (minimum capacitance) and the lowest ratio between the capacitances of the pair of electrodes (1,2) with

the tube filled with the phase of higher relative permittivity and the pair of electrodes (1,5) with the tube filled with a phase of lower relative permittivity.

Table 1 presents the capacitance values as a function of the electrode angle for the geometry of the standard sensor previously described. It can be seen in this table that the highest capacitance value for the pair (1,5) occurs for an electrode angle of 41^o in the case of floating free electrodes and the lowest ratio between the capacitances of the pairs of electrodes (1,2) and (1,5) also occurs for the case of floating free electrodes, however for an electrode angle of 33^o. As the two criteria are met for different angles, the angle of 41^o was chosen because the values of ratio between the capacitances of pairs of electrodes (1,2) and (1,5) for these two angles were very close and the highest capacitance value for the pair of electrodes (1,5) is a very important parameter (little capacitance levels are harder to be measured). Thus are defined the optimized characteristics for the capacitance sensor to be used in the experimental work.

Table 1. Capacitance values (pF) as a function of the electrode angle.

Electrode angle (floating electrodes)	Pair (1,2) with water	Pair (1,5) with air	Ratio between (1,2) and (1,5)
33^0	2.83256	0.11203	25.28
37^0	3.99918	0.14997	26.67
41^0	5.28418	0.19214	27.50

The table 2 summarizes the four basic capacitance values obtained through the numerical simulations for the optimized sensor filled with air and water.

Table 2. Capacitance values (pF) for the sensor filled with air and water.

Pair of electrodes	Air	Water
(1,2)	1.46121	5.28418
(1,3)	0.40044	4.84325
(1,4)	0.22935	4.71215
(1,5)	0.19214	4.67514

CONSTRUCTION OF THE CAPACITANCE SENSIBILITY MAPS

The first step for the two-phase flow image reconstruction consists in the construction of the capacitance sensibility maps, for the air-water flow. The capacitance sensibility of a pixel is a manner of quantify the influence that a specific pixel situated in the interior of a capacitance sensor have over each one of the capacitance values, when only this pixel is occupied by the phase of higher relative permittivity and all other pixels are occupied by the phase of lower relative permittivity.

The detailed procedure for the construction of the capacitance sensibility maps is described in Azevedo Filho (2002).

Figures 5 to 8 present the sensibility maps for air-water flow, for the pairs of electrodes (1,2), (1,3), (1,4) and (1,5). It can be observed that the sensibility is always higher near the electrodes, reducing in the direction to the center of the sensor. It is also observed that the sensibility is higher for the pair of electrodes (1,2) and lower for the pair (1,5).

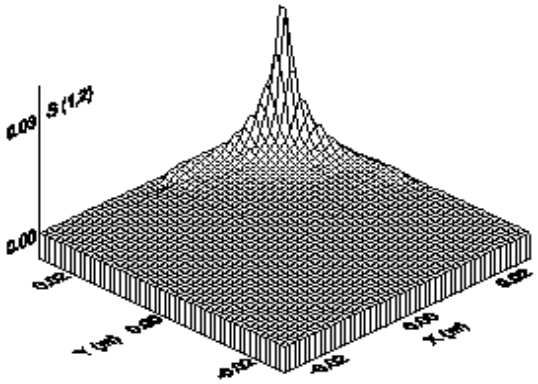

Figure5. Sensibility map of the pair of electrodes (1,2) for air-water

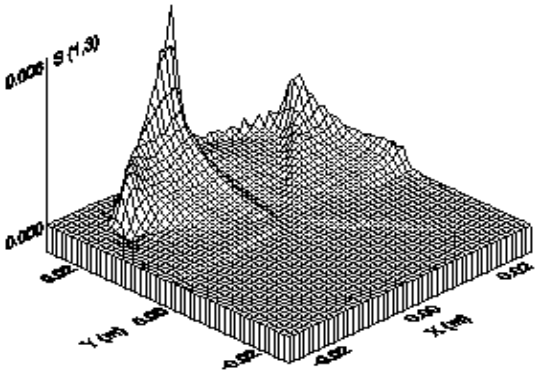

Figure 6. Sensibility map of the pair of electrodes (1,3) for air-water

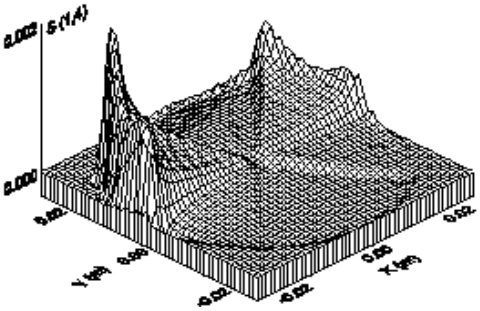

Figure 7. Sensibility map of the pair of electrodes (1,4) for air-water

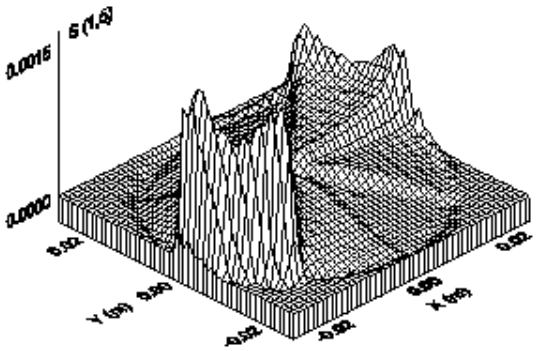

Figure 8. Sensibility map of the pair of electrodes (1,5) for air-water

Results of the image econstruction from the sensibility maps, some images were reconstructed simulating two-phase air-water flow. Images simulating annular and stratified flow patterns were reconstructed. It was used the linear backprojection method for the reconstruction of images, without and with the resource of the cut-off levels, as described above. In this last case was used the input liquid fraction (βv).

The reconstructed images are presented in two manners: s*urface images* that show the behavior of the gray level of the pixels (and the interface between the two phases) and *outline images* showing only the interface between phases. The outline images are bidimensional, therefore, are presented in the *xy* plan without need of change of this plan. For a better view of the interface among the phases, some surface images are showed in different angles

For an air-water flow, the void fraction (α) is defined as the ratio between the area occupied by air and the total internal area of the sensor. Then, the liquid fraction is $\beta = 1 - \alpha$. Figure 9 presents the surface image of an air-water flow, for the annular flow pattern, with a void fraction (α) of 19.05%, using the cut-off level. Figure 10 presents the outline images of the interface for the idealized case (a) and for the simulated case (b). It can be observed in the figure 10 a good agreement of the interface outline between the idealized and simulated cases.

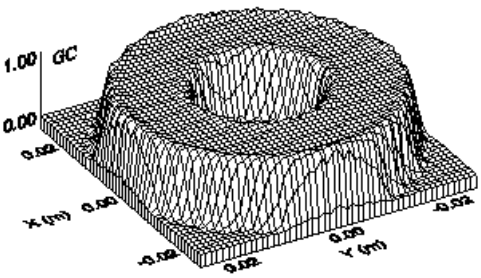

Figure 9. Surface image of an air-water flow in the annular flow pattern, for a void fraction (α) of 19.05%, using the cut-off level resource

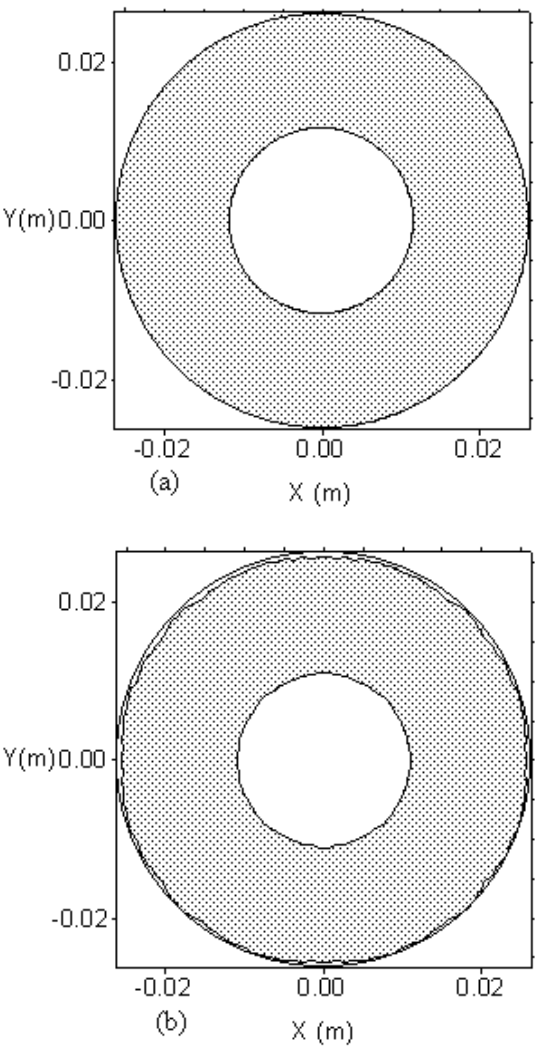

Figure 10. Idealized (a) and simulated (b) outline image of an air-water flow in the annular flow pattern, for a void fraction (α) of 19.05%, using the cut-off level resource

For the stratified air-water flow, images were reconstructed for the values of void fraction of 25,23%, 50.00% and 74.77% using both techniques: without cut-off levels and with cut-off levels. Figures 11 to 16 present the surface images without and with the resource of cut-off level and the idealized and simulated outline images, for the three values of void fraction. Comparing the reconstructed images without and with the cut-off level resources, it can be observed how this resource substantially improves the quality of the images.

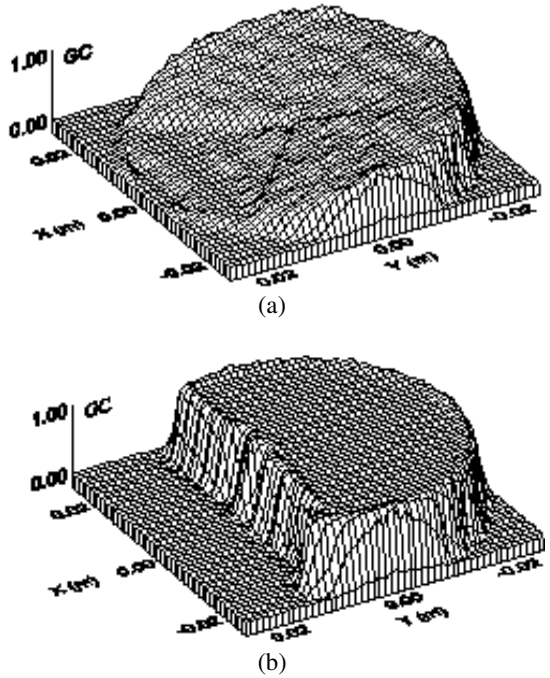

Figure 11. Surface image of an air-water flow in the stratified flow pattern, for a void fraction of 25.23%, without the cut-off level resource (a) and with the cut-off level resource (b)

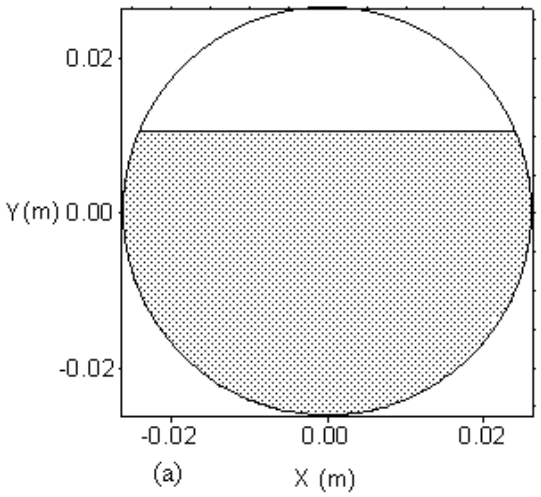

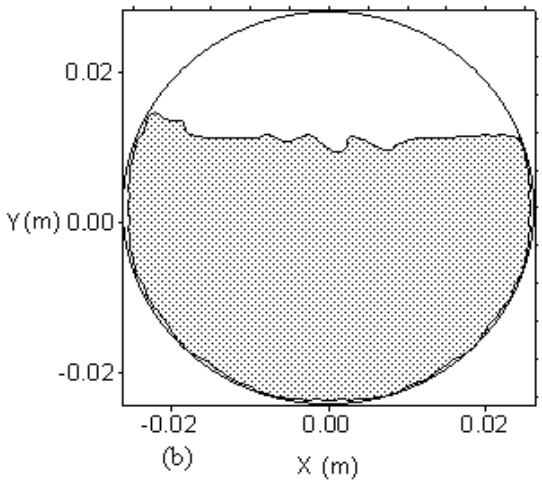

Figure 12. Idealized (a) and simulated (b) outline images of an air-water flow in the stratified flow pattern, for a void fraction of 25.23%, using the cut-off level resource

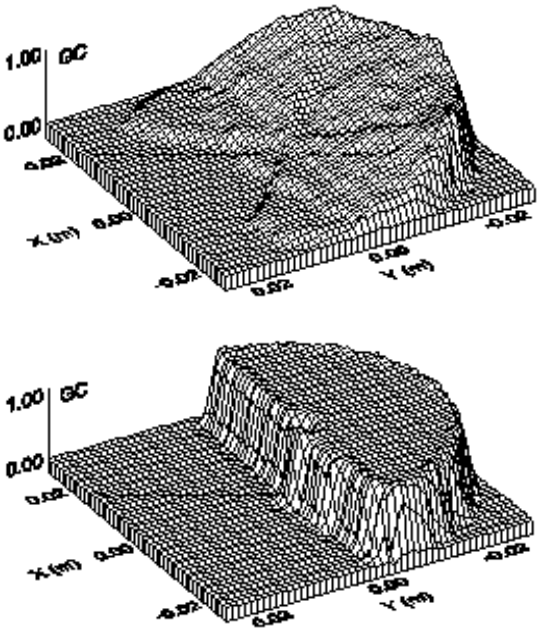

Figure13. Surface images of an air-water flow in the stratified flow pattern, for a void fraction of 50.0%, without the cut-off level resource (a) and with the cut-off level resource (b)

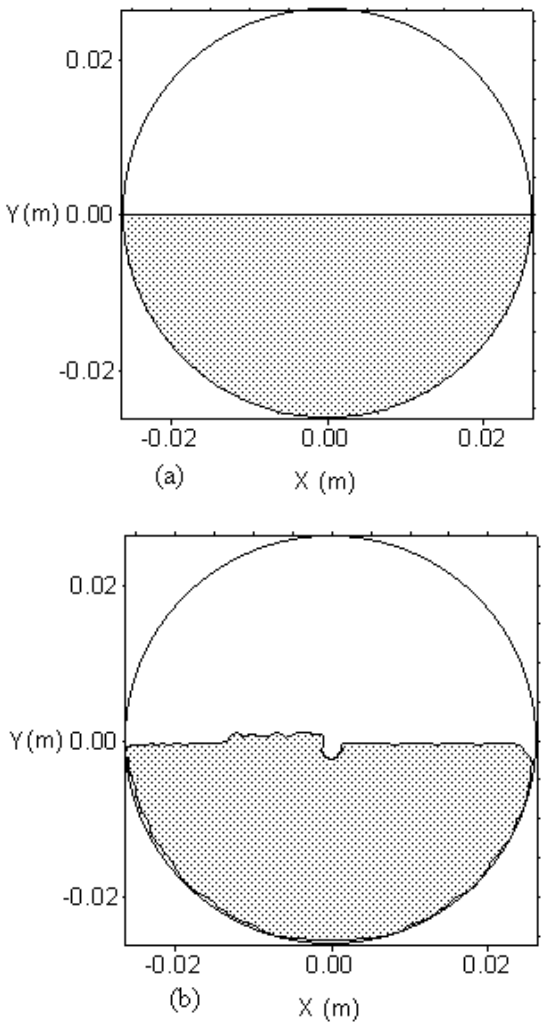

Figure 14. Idealized (a) and simulated (b) outline images of an air-water flow in the stratified flow pattern, for a void fraction of 50.0%, using the cut-off level resource

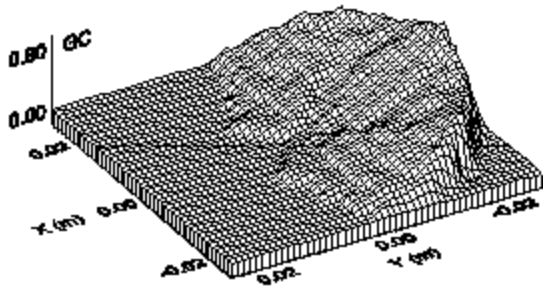

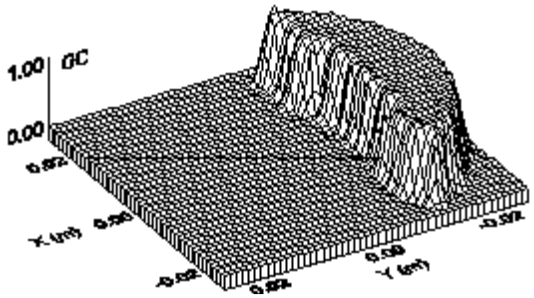

Figure15. Surface images of an air-water flow in the stratified flow pattern, for a void fraction of 74.77%, without the cut-off level resource (a) and with the cut-off level resource (b)

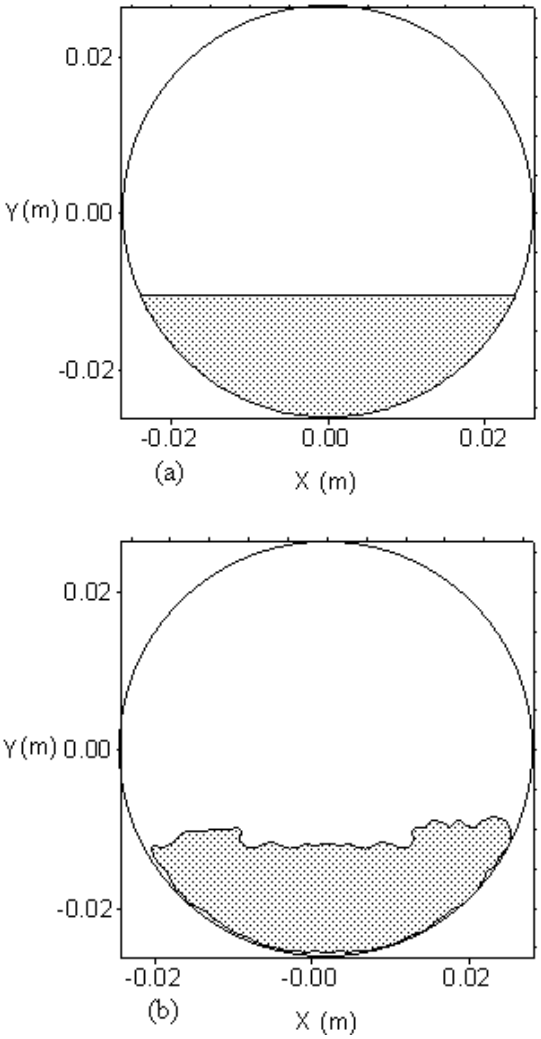

Figure 16. Idealized (a) and simulated (b) outline images of an air-water flow in the stratified flow pattern, for a void fraction of 74.77%, using the cut-off level resource

Analyzing the results presented above it can be observed that, for all simulated cases, the use of the cut-off level resource improves greatly the quality of

the images and allows identifying the interface outline with a reasonable precision. Tables 3 and 4 present the values of input liquid fraction and the simulated liquid fraction obtained without the use of the cut-off level resource. It can be observed that the values of the liquid fraction without cut-off level are discrepant relating to the values of the input liquid fraction. In other words, when the value of the input liquid fraction is not known, it's not possible to correctly identify the interface outline and the value of liquid fraction (obtained without the cut-off level resource) presents certain discrepancy relating to the input value.

Table 3. Values of input liquid fraction (βv) and liquid fraction without cut-off level (βsc) for annular air-water flow

βv	βsc	βv- βsc
0.8095	0.9639	- 0.1544

Table 4. Values of input liquid fraction (βv) and liquid fraction without cut-off level (βsc) for stratified air-water flow

βv	βsc	βv- βsc
0.7477	0.5370	+ 0.2107
0.5000	0.3357	+ 0.1643
0.2523	0.2166	+ 0.0357

CONCLUSIONS

This paper presents the basic concepts related to the electric capacitance tomography for multiphase flows.

Initially, it was performed a numerical study of the parameters that influence the capacitance values between electrodes, in order to obtain an optimized geometry for the capacitance sensor.

The images of the transversal section of two-phase flows were reconstructed from the capacitance values between different pairs of electrodes and from the capacitance sensibility maps, using the linear backprojection algorithm. This algorithm is ease to implement and quick to execute, in such a way that allows the image reconstruction in almost real time.

A resource of cut-off level, which depends on previous knowledge of the liquid fraction, was implemented to improve the quality of the reconstructed images and allow the viewing of the interface between phases.

Images were obtained for two-phase flows of different flow patterns and for several void fraction values. The images obtained represented the flows idealized with quality and clarity, assuring the applicability of the algorithm of linear backprojection. To exemplify the importance of the cut-off level resource, images of some flow patterns were reconstructed without the use of this resource. For all simulated cases, it was observed that the use of the cut-off level resource greatly improves the quality of the images and allows to identify the interface outline with a reasonable precision.

A quantitative analysis also emphasizes the reliability of the linear backprojection algorithm with the resource of cut-off level. This reliability may be verified by the good agreement between the input (real) liquid fraction values and liquid fraction obtained with the use of the resource of cut-off level, for all simulated cases.

Finally, it can be concluded that if the input liquid fraction value is not previously known, it's not possible to correctly identify the interface outline and the value of liquid fraction (obtained without the cut-off level resource) presents certain discrepancy relating to the input value.

REFERENCES

Azevedo Filho, A. C., 2002, Desenvolvimento de um sistema de tomografia capacitiva para processos multifasicos, Doctoral Thesis, Faculdade de Engenharia Mecânica, Universidade Estadual de Campinas.

Belo, F. A., 1995, Aplicação da análise eletrônica ao estudo do escoamento multifásico, Doctoral Thesis, Faculdade de Engenharia Mecânica, Universidade Estadual de Campinas.

Bracewell, R. H., and Riddle, A. C., 1967, Inversion of fan beam scans in radio astronomy, Astrophysics Journal, No. 150, pp. 427-434.

Dykesteen, E. et all, 1985, Non-intrusive three-component ratio measurementment using an impedance sensor, J. Phys. E. Sci. Instrum., No. 18, pp. 540-544.

Fashing, G. E., and Smith Jr., N. S, 1991, A capacitive system for three-dimensional imaging of fluidized beds, Rev. Sci. Instrum., Vol. 62, pp. 2243-2251.

Geldart, D., and Kelsley, J.R., 1972, The use of capacitance probes in gas fluidized beds, Powder Technol. Vol.6, pp. 45-50.

Hage, B., and Werther, J., 1997, The guarded capacitance probe – a tool for the measurementment of solids flow patterns in laboratory industrial fluidized bed combustors, Powder Technol., No. 93, pp. 235-245.

Ishii, M., 1975, Thermo-fluid dynamic theory of two phase flow". Paris: Eyrolles.

McKee, S. L., Williams R. A., Dyakowski, T., and Bell, T. A., 1993, Industrial applications of electrical tomography to conveying processes, Proc. 1993 I Chem. E Res. Event, Birmingham, 6-7 January, Inst. Chem., Eng., pp. 726-728.

Nooralahiyan, A.Y., Hoyle, B.S. and Bailey, N.J., 1993, Application of a neural network in image reconstruction for capacitance topography, Proc. European Concerted Action on Process Topography/UMIST, pp. 144-147.

Ramnchandran, G., and Lakashinarayanan, A. V., 1971, Three dimensional reconstructions from

radiographs and electron micrographs: Application of convolution instead of Fourier transforms, Proceedings of the National Academy of sciences, Vol. 68, pp. 2236-2240.

Strizzolo, C. N., and Convenrti, J., 1993, Capacitance sensors for measurementment of phase volume fraction in two-phase pipeline, IEEE Trans. Instrum. Meas. Vol. 42, No. 3, pp. 726-729.

Xie, C. G. et all., 1993, Review of process topography image reconstruction methods in K.T.V. Grattan and A.T, Augousti (eds). Sensors VI: Technology, Systems and Applications. Bristol: Institute of Physics, pp. 341-346.

Yang, W. Q., and York, T. A., 1999, New AC-based capacitance tomography system, IEE Proc – Sci. Meas. Technol. Vol. 146, No. 1, pp. 47-53.

Received: June 07, 2009
Revised: July 07, 2009
Accepted: August 07, 2009